Highly Efficient Quantum-Dot Light-Emitting Diodes with DNA−CTMA as a Combined Hole-Transporting and Electron-Blocking Layer

Qingjiang Sun,[†] Guru Subramanyam,[†] Liming Dai,[†],* Michael Check,[‡] Angela Campbell,[‡] Rajesh Naik,[‡] James Grote,[‡] and Yongqiang Wang[§]

[†]School of Engineering, University of Dayton, Dayton, Ohio 45469, [‡]Air Force Research Laboratory, Materials and Manufacturing Directorate, AFRL/RX, Wright-Patterson AFB, Ohio 45433, and [§]Ocean NanoTech, LLC, 2143 Worth Lane, Springdale, Arkansas 72764

The recent availability of monodispersed and well-defined colloidal quantum dots (QDs) synthesized from low-cost solution methods has offered a new class of chromophores for the emerging QD-based light-emitting diodes (QD-LEDs) attractive for multiple consumer applications,[1−4] ranging from next-generation user interfaces in mobile devices and personal computers through shadow-less biomedical lamps to flat lighting. Among many advantages of QD chromophores over their organic/polymer counterparts, the main features include their narrow emission bands with a small full width at half-maximum (fwhm <30 nm) and a broad wavelength tunability through the size and/or composition variation(s). In addition, QDs can exhibit a high *photoluminescence* (PL) quantum yield and photochemical stability with appropriate surface functionalization.[2] Recent developments in QD-LEDs have led to bright and color-saturated *electroluminescence* (EL) for the three primary colors[5−7] as well as white light.[7−18] Although all the three primary color QD-LEDs have already shown sufficiently bright electroluminescent emissions (up to ∼9000 cd/m²)[16] required for small-size flat-panel displays (100−500 cd/m²), there is still a pressing need for improving the efficiency of QD-LEDs with a high color purity. This is because even the highest reported external quantum efficiency (EQE) of 2.0% for QD-LEDs[5,15] cannot favorably compete with their highly efficient organic/polymer counterparts.[19] Like polymer LEDs, a balanced injection and confinement of electrons and holes is essential in order to im-

prove the efficiency of QD-LEDs.[18,19] Few of the innovative QD-LED fabrication strategies have been developed, including a phase segregation approach to the monolayer of CdSe/ZnS core/shell QDs[5] and spin-coating QDs directly on the top of a hole transport layer (HTL)[15,16] to improve the brightness[16] and external quantum efficiency.[5] However, most of the reported QD-LEDs suffer from unbalanced charge transport due to the misalignment of their extremely low-lying highest occupied molecular orbits (HOMOs) against those of organic HTLs.[5,16,20] The energy barriers between HTLs and QDs are often further enhanced by the presence of the insulating ligand molecules introduced onto the QD surface during the synthesis for dispersion. So far, no single organic/polymer hole-transporting material has been found to possess HOMO matching that of QDs to enhance the hole transport. Zhao *et al.*[21]

ABSTRACT Owing to their narrow bright emission band, broad size-tunable emission wavelength, superior photostability, and excellent flexible-substrate compatibility, light-emitting diodes based on quantum dots (QD-LEDs) are currently under intensive research and development for multiple consumer applications including flat-panel displays and flat lighting. However, their commercialization is still precluded by the slow development to date of efficient QD-LEDs as even the highest reported efficiency of 2.0% cannot favorably compete with their organic counterparts. Here, we report QD-LEDs with a record high efficiency (∼4%), high brightness (∼6580 cd/m²), low turn-on voltage (∼2.6 V), and significantly improved color purity by simply using deoxyribonucleic acid (DNA) complexed with cetyltrimetylammonium (CTMA) (DNA−CTMA) as a combined hole transporting and electron-blocking layer (HTL/EBL). This, together with controlled thermal decomposition of ligand molecules from the QD shell, represents a novel combined, but simple and very effective, approach toward the development of highly efficient QD-LEDs with a high color purity.

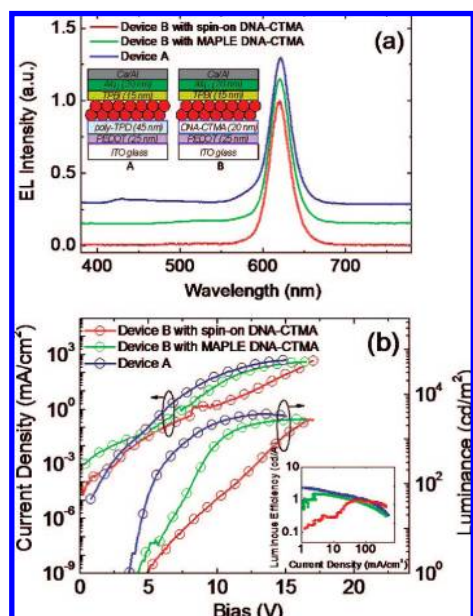**KEYWORDS:** quantum dot · light-emitting diode (LED) · QD-LED · DNA · flat display

Figure 1. (a) EL spectra at a luminance of ~2600 cd/m² and (b) current density−luminance−voltage (*J−L−V*) characteristics for device A with poly-TPD HTL and device B with either spin-on or MAPLE DNA−CTMA HTL. The insets of (a) and (b) show the device configurations and the luminous efficiency *versus* current density curves for devices A and B, respectively.

pioneered an approach to improve the device performance by enhancing the hole transport using two thermally polymerized solvent-resistant HTLs with different HOMOs. While the thermally cross-linked polymers are sufficiently stable to organic solvents used for depositing the top emission layer, the high temperature (typically >250 °C) required for thermal cross-linking could inevitably cause thermal decomposition of the underlying poly(3,4-ethylenedioxythiophene)/poly(styrene-sulfonate) (PEDOT) hole-injection layer (HIL).

In this work, we report a general, but simple and very effective, approach to realizing highly efficient QD-LEDs with a high color purity by using multiple hole-injection (HIL)/HTL layers, composed of PEDOT, poly(*N,N′*-bis(4-butylphenyl)-*N,N′*-bis(phenyl)benzidine (poly-TPD) [or poly(*N*-vinylcarbozole) (PVK) blending with and without poly-TPD], and a salmon-based deoxyribonucleic acid (DNA) complexed with cetyltrimetylammonium (CTMA) to improve the hole transport. It is for the first time that the DNA−CTMA was used in QD-LEDs as both HTL and EBL.[22] The newly developed multiple HIL/HTLs are thermally stable to allow for thermal decomposition of the insulating ligand molecules from the QD shell. As such, efficient and balanced charge transport/confinement can be attained simultaneously, leading to highly efficient QD-LEDs with an excellent color purity. As we shall report, QD-LEDs developed in this study are characterized by a very low turn-on voltage (~2.6 V), high brightness (~6580 cd/m²), high efficiency (~4 cd/A), and significantly improved color purity.
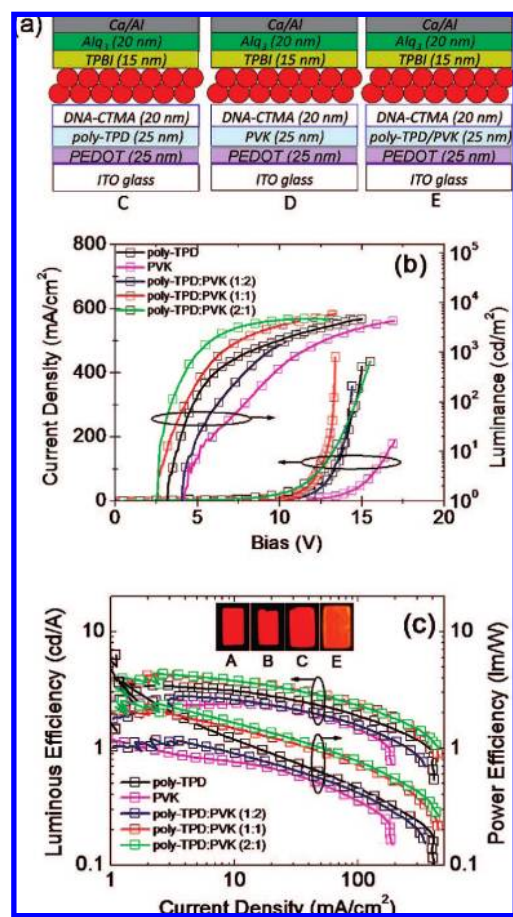

Figure 2. (a) Schematic device configurations, (b) *J−L−V* characteristics, and (c) luminous efficiency and power efficiency *versus* current density curves for devices C, D, and E with multiple HIL/HTLs. The insets of (c) show the photos of devices A, B, C, and E operated at a constant current density of 10 mA/cm². The figure legends in (b) and (c) represent the compositions of the second HTL used in those devices shown in (a).

As double-shell QDs often exhibit higher PL quantum yields than their single-shell counterparts, we used CdSe/CdS/ZnS (core/shell/shell) QDs with an average diameter of ~8 nm in this study. The core/shell/shell structure can further facilitate the charge injection from organic HTLs/ETLs to QDs through the gradient energy levels from the ZnS outer-shell through the CdS inner-shell to the CdSe core. In a typical experiment, the QDs were washed at least three times to remove excess ligand molecules and/or impurities. Sun *et al.*[16] have previously demonstrated that QD-LEDs constructed from these purified QDs showed better performance than those based on the as-prepared QDs, though the purification process could significantly reduce the PL quantum yield from ~80 to 30%. The purified CdSe/CdS/ZnS QDs showed saturated red PL emission peaked at ~610 nm with the fwhm of ~24 nm.

Five-layer QD-LEDs with either poly-TPD (device A) or DNA−CTMA (device B) as the HTL (inset of Figure 1a) were fabricated. In both devices, PEDOT was spin-coated from its aqueous solution as a HIL to increase
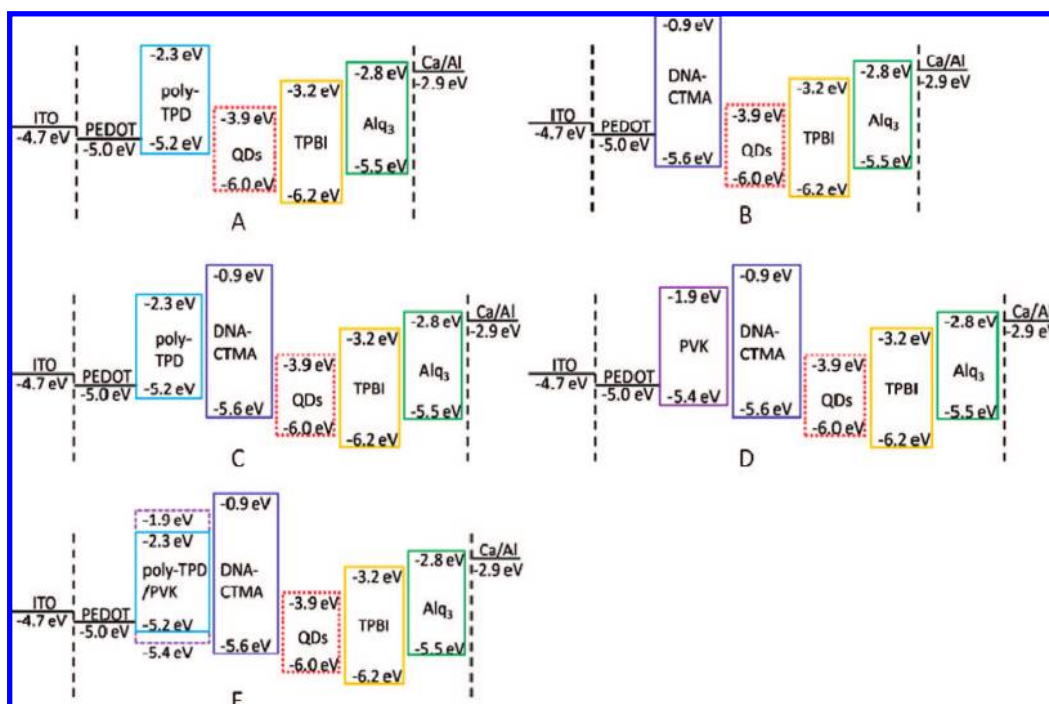
Figure 3. Schematic energy level diagrams for the materials involved in devices A−E.

the work function of an indium−tin−oxide (ITO) anode from 4.7 to 5.0 eV and to reduce surface roughness for stable and pinhole-free electrical conduction.[23,24] The QD layer (~2 monolayers) was prepared by spin-coating its toluene solution of an optical density (O.D. ≈ 2) at 1500 rpm, followed by drying at 80 °C for 10 min. ETLs were then prepared by sequential thermal deposition of 1,3,5-tris(N-phenylbenzimidazol-2-yl)benzene (TPBI) and tris(8-hydroxyquinoline)-aluminum (Alq₃) under high vacuum. For device A, the HTL was prepared by spin-coating a chlorobenzene solution of poly-TPD onto the PEDOT layer, followed by annealing at 150 °C for 30 min. For device B, the DNA−CTMA layer was formed by either spin-coating from a butanol solution (2 mg/mL) at 4000 rpm or through a matrix-assisted pulse laser evaporation (MAPLE) process (see Methods). The selective solubility of DNA−CTMA in alcohol allowed its film formation by spin-coating without dissolving the underlying HIL (PEDOT)/organic HTLs. On the other hand, the DNA−CTMA layer, once formed either by spin-coating or MAPLE, was free from damage by organic solvents (e.g., toluene) used for casting the overlaid QD layer due to its selective solubility in alcohols. These DNA−CTMA HTLs/EBLs possess unique optoelectronic properties,[22−26] including their optical transparency and relatively low/high HOMO/LUMO (−5.6/−0.9 eV) attractive for the energy level adjustment in QD-LEDs described below.

Figure 1a shows the electroluminescent (EL) spectra for device A and device B with either spin-on or MAPLE DNA−CTMA under high brightness (voltage). All devices showed that saturated red emission from

CdSe/CdS/ZnS peaked at ~621 nm with the fwhm of ~28 nm. The small red shift observed for EL relative to PL is attributable to Förster energy transfer and/or the Stark effect.[12] The deep blue EL emission from poly-TPD having a band gap of 2.9 eV in device A was observed at ~420 nm under a brightness of ~2600 cd/m² as electrons on the LUMO of TPBI could jump over the 0.9 eV energy barriers into the LUMO of poly-TPD through defects of the QD layer (only ~2 monolayers) to combine with holes in the poly-TPD layer (see Figure 3A). For the devices containing either spin-on or MAPLE DNA−CTMA, with a wide band gap of 4.7 eV, however, no EL emission from the HTL/ETL was observed even at a high brightness as electrons from TPBI were completely blocked by the DNA−CTMA EBL before jumping into the LUMO of poly-TPD (see Figure 3B). This is another important advantage of the DNA−CTMA QD-LEDs as the blue emission from poly-TPD degrades the color purity. The Commission Internationale de L'Eclairage (CIE) coordinates[27] for the light emitted from device B are (0.68, 0.31), which exceeds the high-definition television (HDTV) standard for red emission.

Figure 1b shows typical current density−luminance−voltage (J−L−V) characteristics for devices A and B. Also included in the inset of Figure 1b is the corresponding EL efficiency as a function of the current density. As can be seen, device B with MAPLE DNA−CTMA exhibited overwhelmingly better performance than that with the spin-on DNA−CTMA. Overall, device A displayed better performance than device B. Table lists the turn-on voltage (V_{on}), the maximum luminance (L^{max}), and the maximum luminous efficiency (LE^{max}) for devices A and B (other devices are discussed
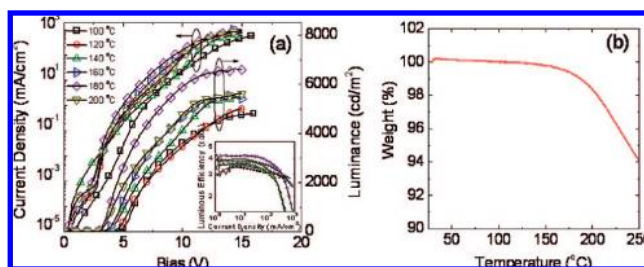
Figure 4. (a) The $J-L-V$ characteristics of device C with QDs having been annealed at different temperatures for 10 min. The inset of (a) shows the corresponding luminous efficiency *versus* current density curves. (b) Thermogravimetric analysis of CdSe/CdS/ZnS core/shell/shell QDs on the ITO/PEDOT/poly-TPD/DNA-CTMA multilayer.

later). The observed difference in device performance for device B with the DNA−CTMA thin films deposited by spin-coating *versus* MAPLE most probably originated from different hole-transporting capabilities of the DNA−CTMA films related to different impurity levels, as both the spin-cast and MAPLE DNA−CTMA films possess the same film thickness (20 nm) and QD distribution with a similar surface morphology (Figure S1 in the Supporting Information). However, the high-vacuum MAPLE process is believed to produce a relatively pure DNA−CTMA thin film with a well-defined molecular weight in respect to spin-coating.[26]

In order to further improve the EL efficiency, six-layer QD-LEDs based on trilayer HIL/HTLs were fabricated with the MAPLE DNA−CTMA being used as the underlying HTL for the QD emitters (Figure 2a). The second HTLs in devices C, D, and E were poly-TPD, PVK, and poly-TPD/PVK blends (weight ratios of 1:2, 1:1, and 2:1), respectively, spin-cast from the corresponding chlorobenzene solutions (PVK is another well-known hole-transporting polymer in organic/polymer LEDs[17]). The $J-L-V$ characteristics, luminous and power efficiencies for devices C, D, and E are given in Figure 2b,c. As can be seen, the device performance strongly depends on the compositions of the HIL/HTL layers. Device C, with a combined poly-TPD/DNA−CTMA HTL, showed much better performance than devices A and B (Table). Using PVK/DNA−CTMA as the combined HTLs, device D exhibited reduced outputs with respect to device C (Table). The performance of device E varied with poly-TPD/PVK weight ratios in the first HTL. Device E, with a poly-TPD/PVK weight ratio of 1:2, showed a worse overall performance than that of device C (1). By increasing the poly-TPD/PVK weight ratios up to 1:1

and 2:1, however, we observed an improved overall performance than that of device C for device E; a V_{on} of 2.6 V, L^{max} of ~5250−5760 cd/m^2, LE^{max} of 4.3 cd/A, and PE^{max} of 2.1−2.3 lm/W. The inset of Figure 2c shows the photos of devices A, B, C, and E operated at a constant current density of 10 mA/cm^2. These devices exhibited different light outputs at the same current density due to different efficiencies.

The device performance variations described above for all of the QD-LEDs investigated in this study can be rationalized by the schematic energy level diagrams shown in Figure 3. As mentioned earlier, PEDOT acts as the HIL in all devices by improving the work function of ITO from −4.7 to −5.0 eV. With its HOMO (−5.2 eV) close to the work function of PEDOT HIL and its LUMO (−2.3 eV) being 1.6 eV higher than that of QDs (−3.9 eV) and 0.9 eV higher than that of TPBI ETL (−3.2 eV),[17,28,29] poly-TPD may act as HTL/EBL in device A. Similarly, DNA−CTMA acts as the HTL/EBL in device B since its HOMO (−5.6 eV) lies between the work function of PEDOT HIL and the HOMO of QDs (−6.0 eV)[16] and its LUMO (−0.9 eV) is 3 eV higher than that of QDs and 2.3 eV higher than that of TPBI.[22,25,26] The energy barrier of 2.3 eV between the LUMO of DNA−CTMA and that of TPBI is too high for electrons to reach the DNA−CTMA layer from the TPBI layer in device B, though the electrons on LUMO of TPBI in device A can overcome the 0.9 eV energy barriers to jump into the LUMO of poly-TPD to produce the blue emission from poly-TPD under high voltages (*vide supra*). Consequently, device B exhibited a higher EL color purity than device A. The better overall performance achieved from device A compared to device B indicates a higher overall hole-transporting capability for poly-TPD than DNA−CTMA.[30] Nevertheless, a balanced hole and/or electron transport has not yet been achieved for device A nor for device B. As seen in Figure 3, the transport of electrons from the Ca/Al cathode to the LUMO of QDs in both devices is in cascade through the LUMOs of Alq$_3$ and TPBI ETLs. On the other hand, the holes injected from the ITO anode in device A can transport easily to the HOMO of poly-TPD HTL through PEDOT HIL but may accumulate at the poly-TPD/QD interface with an energy barrier of 0.8 eV. In device B, the holes need to first overcome a relatively high energy barrier of 0.6 eV to inject from PEDOT HIL to the HOMO of DNA−CTMA and then an additional 0.4 eV to the HOMO of QDs.

The above discussion indicates that holes are minority carriers and electrons are majority carriers in these QD-LEDs, which is opposite to most organic/polymer light-emitting devices, given that most organic molecules/polymers are p-type semiconductors.[18] In order to improve EL efficiency, it is important to enhance the injection/transport of minority carriers. The high efficiency of the six-layer QD-LEDs, with the DNA−CTMA HTL/EBL, is thus attributable to the improved hole

TABLE 1. EL Performance of the QD-LEDs Constructed in this Study

		device B		device C	device D	device E	
	deviceA	spin-on	MAPLE			1:2^a	1:1−2:1^a
V_{on} (V)	3.6	5.0	4.2	3.2	4.2	4.0	2.6
L^{max} (cd/m^2)	~3610	~2724	~2758	~4737	~4278	~4749	~5250−5760
LE^{max} (cd/A)	2.4	1.0	1.5	3.4	2.4	2.8	4.3
PE^{max} (lm/W)				1.8	0.8	1.5	2.1−2.3

^{a}The poly-TPD/PVK weight ratios.

TABLE 2. EL of Device C after Thermal Annealing at Different Temperatures for 10 min

	device C				
	80—100 °C	120 °C	140—160 °C	180 °C	200 °C
V_{on} (V)	3.2	3.2	2.9	2.6	2.6
L^{max} (cd/m^2)	~4737	~5000	5400—5700	~6580	~5800
LE^{max} (cd/A)	3.4	3.5	3.7 — 3.8	4.1	3.9

transport efficiency. Compared to device A, the 0.8 eV energy barrier between HOMOs of poly-TPD and QDs (Figure 3A) is alleviated by the in-between DNA—CTMA HTL in device C for an easy hole transport to the HOMO of QDs from that of the poly-TPD HTL through the HOMO of DNA—CTMA by overcoming energy barriers of only 0.4 eV on both sides of the DNA—CTMA layer (Figure 3C). Compared to device B, the 0.6 eV energy barrier between the work function of PEDOT and the HOMO of DNA—CTMA (Figure 3B) is alleviated by the in-between poly-TPD HTL in device C to be 0.2 and 0.4 eV energy barriers on each side of the poly-TPD layer (Figure 3C). Therefore, device C exhibited an improved overall performance than both device A and device B while retaining the high color purity (Table). Although PVK has a HOMO of −5.4 eV, aligning well with that of DNA—CTMA, the overall performance for device D is lower (an increased V_{on} and decreased L^{max}, LE^{max}, and PE^{max}) than that of device C (Table), indicating that the hole-transporting capability of PVK is not as good as that of poly-TPD. In device E, the transport of holes from the PEDOT HIL to DNA—CTMA HTL is believed to be multichanneled, as holes can simultaneously inject into the HOMOs of poly-TPD and PVK from the PEDOT HIL, followed by subsequent transport into the HOMO of DNA—CTMA. For hole transport through the first HTL in device E, part of the holes in the HOMO of poly-TPD may first go to the HOMO of PVK (0.2 eV lower than that of poly-TPD) and then transport to the HOMO of DNA—CTMA. In this case, the 0.4 eV energy barrier between the work function of PEDOT and the HOMO of PVK is alleviated by the intermixed poly-TPD HTL, while the 0.4 eV energy barrier between HOMOs of poly-TPD and DNA—CTMA is also alleviated by the intermixed PVK HTL (Figure 3E). At a poly-TPD/PVK weight ratio of 1:2, the hole transport through PVK is dominant with the hole injection from PEDOT HIL into the HOMO of PVK being only slightly improved by the relatively small amount of the intermixed poly-TPD, leading to a better device performance of device E than device D, but worse than device C (Table). Upon increasing the poly-TPD/PVK weight ratios up to 1:1 and 2:1, the multichanneled hole transport from PEDOT HIL to DNA—CTMA HTL, through poly-TPD/PVK, and then to QDs is optimized. Device E, thus, exhibited a better performance than that of device C (Table).

In addition to the engineering of the HIL/HTLs described above, we also exploited *in situ* ligand decom-

position to further improve the device performance. The coverage of QD core/shell by insulating ligands is known to be necessary for uniform dispersion of QDs in solution and uniform film formation for device applications. However, the presence of these insulating ligand molecules around the QD shell could inevitably cause an additional energy barrier for the carrier injection from HTLs and ETLs to the QD core. It has recently been reported that enhanced performance of QD-LEDs could be achieved by high-temperature thermal annealing of QDs on a cross-linked polymer HTL to decompose ligand molecules from the QD shell.[15] Therefore, device C was chosen to investigate possible thermal effects on the device performance as PVK is susceptible to thermal degradation (Figure S2 in the Supporting Information). Figure 4a shows the J−L−V characteristics for device C after being annealed at different temperatures between 100 and 200 °C for 10 min. Also included in the inset of Figure 4a are the corresponding curves for the luminous efficiencies *versus* current densities. As can be seen, the device with QDs annealed at temperatures be-
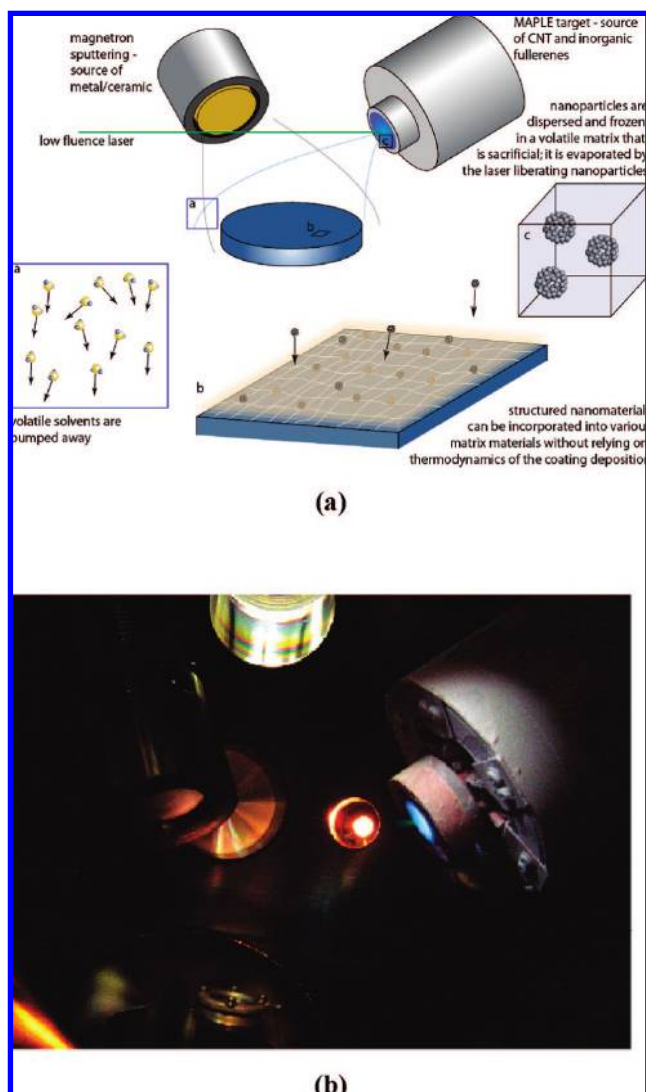

Figure 5. MAPLE deposition system: (a) schematic and (b) photograph.

low 120 °C exhibited similar performance to the as-prepared device C (annealed at 80 °C, Figure 2b,c). Upon increasing the annealing temperature up to and above 140 °C, the device performance was significantly improved as reflected by a reduced V_{on} and an increased L^{max} and LE^{max} (TableTable). For instance, the device with QDs annealed at 120 °C showed a V_{on} of ~3.2 V, L^{max} of ~5000 cd/m^2, and LE^{max} of 3.5 cd/A, while the device with QDs annealed at 180 °C achieved the best performance with a V_{on} of 2.6 V, L^{max} of ~6580 cd/m^2, and the LE^{max} of ~4.1 cd/A. Although devices with QDs annealed at 200 and 180 °C turned on at a similar V_{on} of 2.6 V, the former showed a reduced L^{max} of 5800 cd/m^2 and LE^{max} of 3.9 cd/A.

Comparing Figure 4a with Figure 2b indicates that the enhanced device performance induced by the high-temperature annealing (≥140 °C) arises from an increased current injection due to the thermal decomposition of ligand molecules from the QD shell. This is further supported by the thermogravimetric analysis (TGA) result for the CdSe/CdS/ZnS QDs given in Figure 4b, which shows a noticeable weight loss of ~0.11% over ~120−180 °C, reflecting the gradual decomposition of ligand molecules from the QD shell.[22] The further weight loss observed above 180 °C is, most probably, due to the excess loss of the surface-bound ligands accompanied by thermal decomposition of other organic components within the device structure (e.g., DNA−CTMA, poly-TPD; Figure S2 in Supporting Information). The ligand decomposition facilitates the carrier injection from HTLs and ETLs to the QD core and also increases the interdot carrier mobility, leading to the enhanced device performance for the thermally annealed QD-LEDs. However, the thermal annealing was found to be accompanied by a concomitant film morphology change that could inevitably cause some detrimental effects to the device performance. As a result, device C, with QDs being annealed at 200 °C, showed an overall decrease in the device performance, due to the increased surface roughness caused by reaggregation of QDs, after the excess loss of surface bound ligands in this particular case, and possible thermal decomposition of certain organic components within the device structure (Figures S2 and S3 in the Supporting Information).

In summary, we have demonstrated that the use of DNA−CTMA as a combined HTL and EBL, coupled with controlled thermal annealing to decompose ligand molecules from the QD shell, can significantly enhance the device performance, including the color purity, of QD-LEDs through efficient, but balanced, carrier injection/transport and strong charge confinement. QD-LEDs with a record high efficiency, high brightness, low turn-on voltage, and improved color purity have been successfully demonstrated. The methodology developed in this study represents a significant advance in the development of highly efficient QD-LEDs with an excellent color purity for various applications, such as in the next generation of flat-panel displays and flat lighting systems.

METHODS

Materials. Poly(3,4-ethylenedioxythiophene)/poly(styrene-sulfonate) (PEDOT) was supplied by Baytron (Al P4083), while poly(N,N′-bis(4-butylphenyl)-N,N′-bis(phenyl)benzidine (poly-TPD, ADS 254BE) and poly(N-vinylcarbozole) (PVK) were purchased from American Dye Source, Inc. and Aldrich, respectively. 1,3,5-Tris(N-phenylbenzimidazol-2-yl)benzene (TPBI) and tris(8-hydroxyquinoline)aluminum (Alq$_3$) were obtained from H.W. Sands Corp. The CdSe/CdS/ZnS QDs were provided by Ocean NanoTech, LLC. All chemicals were used without further purification unless otherwise stated.

Formation of the DNA−CTMA Layer. DNA−CTMA complexes for solution spinning were prepared according to the reported procedure.[31] Briefly, 4 g of the pristine DNA sample ($M_w \approx 8000$ kDa) provided by the Chitose Institute for Science and Technology (CIST) was dissolved in 1 L of 14 MΩ·cm distilled/deionized water at room temperature. The DNA solution was then sonicated at 0 °C with 10 and 20 s durations for each of the sonication wave pulses and between the pulses, respectively, to reduce the molecular weight of DNA to ~200 kDa. This was followed by filtration through a nylon filter with a 0.45 μm pore size to remove any particles created during sonication. The filtered DNA solution was then added dropwise to an equal amount of CTMA solution (4 g/L in 14 MΩ·cm distilled/deionized water) with a burette. White DNA−CTMA precipitates formed as the DNA was added to the aqueous solution of CTMA. After having mixed the solution for an additional 4 h at room temperature, the precipitate was removed by filtering the solution under a vacuum using a nylon filter with a pore size of 20 μm. During the filtering process, an additional 3−4 L of 14 MΩ·cm distilled/deionized water was poured through the filter to rinse the precipitate and to ensure that any CTMA that did not bind to the DNA was thoroughly rinsed away. The precipitate was then collected, placed in a Teflon beaker, and dried in a vacuum oven overnight at 40 °C. The resultant DNA−CTMA complexes were found to be soluble in alcohol but not in water or other common organic solvents for solution-spinning into thin films.

Alternatively, matrix-assisted pulsed laser evaporation (MAPLE) was explored for deposition of the DNA−CTMA layer.[26] Figure 5 shows the schematic and photograph of the MAPLE process. As can be seen, MAPLE is a modified pulsed laser deposition technique that involves laser ablation of a target prepared by dissolving organic material(s) in an appropriate solvent and freezing the solution solid with liquid nitrogen. The solvent (i.e., butanol in this case) in the resulting solid matrix target evaporates when exposed to excimer laser pulses, while the organic material(s) is released and deposited onto the desired substrate. Unlike conventional pulsed laser deposition (PLD) techniques, the organic materials in resulting films deposited by MAPLE retain their chemical and structural integrity. It is considered a pseudodry technique where the organic material(s) behaves as though it was deposited by a physical deposition process. MAPLE produces high quality, highly uniform, adherent, organic, polymeric, biopolymer, and inorganic polymer thin films on many different types of substrates of varying geometries. The technique provides precise uniform thickness control, multilayer capability, discrete deposition of materials and uniform conformal coverage. MAPLE has been used for fabrication of thin films for various applications, such as chemical and biological sensors, microfluidic biosensors, biocompatible polymer films for drug-delivery systems, DNA and antibody microarrays, and biocompatible coatings for implants and pharmaceutical applications.

Charaterization. Electroluminescence (EL) spectra were recorded with an Ocean Optics USB-4000 optical fiber. The current−voltage (J−V) and luminance−voltage (L−V) characteristics were measured on a computer-controlled Keithley 236 Source-Measure Unit and a Keithley 2000 Multimeter coupled with a Si photomultiplier tube. The absolute light intensity was calibrated by a Minolta LS-110 camera. All the measurements were performed under ambient conditions.

Supporting Information Available: Surface morphology of DNA−CTMA layers and thermal annealing of the QD-LEDs. This material is available free of charge *via* the Internet at http://pubs.acs.org.

REFERENCES AND NOTES

1. Talapin, D. V.; Mekis, I.; Goetzinger, S.; Kornowski, A.; Benson, O.; Weller, H. CdSe/CdS/ZnS and CdSe/Znse/ZnS Core−Shell−Shell Nanocrystals. *J. Phys. Chem. B* **2004**, *108*, 18826–18831.

2. Xie, R.; Kolb, U.; Li, J.; Basche, T.; Mews, A. Synthesis and Characterization of Highly Luminescent CdSe-Core CdS/Zn0.5Cd0.5S/ZnS Multishell Nanocrystals. *J. Am. Chem. Soc.* **2005**, *127*, 7480–7488.

3. Li, J. J.; Wang, Y. A.; Guo, W.; Keay, J. C.; Mishima, T. D.; Johnson, M. B.; Peng, X. Large-Scale Synthesis of Nearly Monodisperse CdSe/CdS Core/Shell Nanocrystals Using Air-Stable Reagents *via* Successive Ion Layer Adsorption and Reaction. *J. Am. Chem. Soc.* **2003**, *125*, 12567–12575, and references cited therein. .

4. Bruchez, M.; Moronne, M.; Gin, P.; Weiss, S.; Alivisatos, A. P. Semiconductor Nanocrystals as Fluorescent Biological Labels. *Science* **1998**, *281*, 2013–2016.

5. Coe-Sullivan, S.; Woo, W.-K.; Bawendi, M.; Bulovic, V. Electroluminescence from Single Monolayers of Nanocrystals in Molecular Organic Devices. *Nature* **2002**, *420*, 800–803.

6. Steckel, J. S.; Zimmer, J. P.; Coe-Sullivan, S.; Stott, N. E.; Bulovic, V.; Bawendi, M. Blue Luminescence from (CdS)ZnS Core−Shell Nanocrystals. *Angew. Chem., Int. Ed.* **2004**, *43*, 2154–2158.

7. Steckel, J. S.; Snee, P.; Coe-Sullivan, S.; Zimmer, J. P.; Halpert, J. E.; Anikeeva, P.; Kim, L.; Bulovic, V.; Bawendi, M. G. Color-Saturated Green-Emitting QD-LEDs. *Angew. Chem., Int. Ed.* **2006**, *45*, 5796–5799.

8. Li, Y.; Rizzo, A.; Mazzeo, M.; Carbone, L.; Manna, L.; Cingolani, R.; Gigli, G. White Organic Light-Emitting Devices with CdSe/ZnS Quantum Dots as A Red Emitter. *J. Appl. Phys.* **2005**, *97*, 113501-1–113501-4.

9. Anikeeva, P. O.; Halpert, J. E.; Bawendi, M. G.; Bulovic, V. Electroluminescence from a Mixed Red-Green-Blue Colloidal Quantum Dot Monolayer. *Nano Lett.* **2007**, *7*, 2196–2200.

10. Kumar, N. D.; Joshi, P. M.; Friend, C. S.; Prasad, P. N.; Burzynski, R. Organic−Inorganic Heterojunction Light Emitting Diodes Based on Poly(*p*-phenylene vinylene)/Cadmium Sulfide Thin Films. *Appl. Phys. Lett.* **1997**, *71*, 1388–1390.

11. Schlamp, M. C.; Peng, X.; Alivisatos, A. P. Improved Efficiencies in Light Emitting Diodes Made with Cdse(Cds) Core/Shell Type Nanocrystals and a Semiconducting Polymer. *J. Appl. Phys.* **1997**, *82*, 5837–5842.

12. Zhao, J. L.; Zhang, J.; Jiang, C; Bohnenberger, J; Basche, T; Mews, A. Electroluminescence from Isolated CdSe/ZnS Quantum Dots in Multilayered Light-Emitting Diodes. *J. Appl. Phys.* **2004**, *96*, 3206–3210.

13. Jun, S.; Jang, E.; Park, J.; Kim, J. Photopatterned Semiconductor Nanocrystals and Their Electroluminescence from Hybrid Light-Emitting Devices. *Langmuir* **2006**, *22*, 2407–2410.

14. Ginger, D. S.; Greenhama, N. C. Charge Injection and Transport in Films of CdSe Nanocrystals. *J. Appl. Phys.* **2000**, *87*, 1361–1368.

15. Niu, Y.; Munro, A. M.; Cheng, Y.; Tian, Y.; Liu, M. S.; Zhao, J. L.; Bardecker, J. A.; Plante, I. J.; Ginger, D. S.; Jen, A. K. Improved Performance from Multilayer Quantum Dot Light-Emitting Diodes *via* Thermal Annealing of the Quantum Dot Layer. *Adv. Mater.* **2007**, *19*, 3371–3376.

16. Sun, Q. J.; Wang, Y. A.; Li, L.; Wang, D.; Zhu, T.; Xu, J.; Yang, C.; Li, Y. F. Bright, Multicoloured Light-Emitting Diodes Based on Quantum Dots. *Nat. Photonics* **2007**, *1*, 717–722.

17. Sun, Q. J.; Hou, J. H.; Yang, C. H.; Li, Y. F.; Yang, Y. Enhanced Performance of White Polymer Light-Emitting Diodes Using Polymer Blends as Hole-Transporting Layers. *Appl. Phys. Lett.* **2006**, *89*, 153501-1–153501-3.

18. Dai, L. *Intelligent Macromolecules for Smart Devices: From Materials Synthesis to Device Applications*; Springer: Berlin, 2004.

19. *Organic Light-Emitting Devices: Synthesis, Properties, and Applications*; Mullen, K., Scherf, U., Eds.; Wiley-VCH: Weinheim, Germany, 2006.

20. For QDs with the low-lying HOMOs and LUMOs, electrons could be injected from the cathode into the LUMO of QDs in cascade through that of an ETL, whereas the holes injected from an anode into the HOMO of a HTL might be unable to reach that of QDs due to a high energy barrier at the HTL/QD interface for the hole transport.

21. Zhao, J.; Bardecker, J. A.; Munro, A. M.; Liu, M. S.; Niu, Y.; Ding, I.-K.; Luo, J.; Chen, B.; Jen, A. K.-Y.; Ginger, D. S. Efficient CdSe/CdS Quantum Dot Light-Emitting Diodes Using a Thermally Polymerized Hole Transport Layer. *Nano Lett.* **2006**, *6*, 463–467.

22. Steckl, A. J. DNA? A New Material for Photonics? *Nat. Photonics* **2007**, *1*, 3–5.

23. Carter, J. C.; Grizzi, I.; Heeks, S. K.; Lacey, D. J.; Latham, S. G.; May, P. G.; Delospanos, O. R.; Pichler, K.; Towns, C. R.; Wittmann, H. F. Operating Stability of Light-Emitting Polymer Diodes Based on Poly(*p*-phenylene vinylene). *Appl. Phys. Lett.* **1997**, *71*, 34–36.

24. Brown, T. M.; Kim, J. S.; Friend, R. H.; Cacialli, F.; Daik, R.; Feast, W. J. Built-in Field Electroabsorption Spectroscopy of Polymer Light-Emitting Diodes Incorporating A Doped Poly(3,4-ethylene dioxythiophene) Hole Injection Layer. *Appl. Phys. Lett.* **1999**, *75*, 1679–1681.

25. Hagen, J.; Li, W.; Grote, J.; Steckl, A. Enhanced Emission Efficiency in Organic Light-Emitting Diodes Using Deoxyribonucleic Acid Complex as an Electron Blocking Layer. *Appl. Phys. Lett.* **2006**, *88*, 171109-1–171109-3.

26. Hagen, J.; Li, W.; Spaeth, H.; Grote, J.; Steckl, A. Molecular Beam Deposition of DNA Nanometer Films. *Nano Lett.* **2007**, *7*, 133–137.

27. http://www.ph.tn.tudelft.nl/Courses/FIP/noframes/fip-Color.html.

28. Grice, A. W.; Bradley, D. D. C.; Bernius, M. T.; Inbasekaran, M.; Wu, W. W.; Woo, E. P. High Brightness and Efficiency Blue Light-Emitting Polymer Diodes. *Appl. Phys. Lett.* **1998**, *73*, 629–631.

29. Sun, Q. J.; Fan, B. H.; Tan, Z. A.; Yang, C. H.; Li, Y. F.; Yang, Y. White Light from Polymer Light-Emitting Diodes: Utilization of Fluorenone Defects and Exciplex. *Appl. Phys. Lett.* **2006**, *88*, 163510-1–163510-3.

30. Sun, Q. J.; Chang, D.; Dai, L.; Grote, J.; Naik, R. Multilayer White Polymer Light-Emitting Diodes with Deoxyribonucleic Acid−Cetyltrimetylammonium Complex as a Hole-Transporting/Electron-Blocking Layer. *Appl. Phys. Lett.* **2008**, *92*, 251108-1–251108-3.

31. Heckman, E; Hagen, J; Yaney, P; Grote, J; Hopkins, F. Processing Techniques for Deoxyribonucleic Acid: Biopolymer for Photonics Applications. *Appl. Phys. Lett.* **2005**, *87*, 211115.